Journal of Statistical Physics, Vol. 62, Nos. 5/6, 1991

Rheology of Nematic Solutions of Rodlike Chains: Comparison of Theory and Experiment

G. C. Berry[1] and Mohan Srinivasarao[1]

Received Octobet 28, 1989; final March 27, 1990

The rheological properties of nematic solutions of rodlike polymers are discussed, giving comparisons between theoretical results and certain experiments. Most of the theoretical treatments are based on application of the Leslie–Ericksen constitutive equation. The experimental data considered include distortion in a magnetic field and flow in shearing deformation over a range of shear rate, including rheo-optical observations. In general, it appears that the available theory does not describe a number of the features observed.

KEY WORDS: Nematic; rodlike polymer; rheology; rheo-optical.

1. INTRODUCTION

The properties of nematic solutions of rodlike chains pose interesting and difficult problems owing to the long coherence length for orientational correlation among the chain axes, and the resulting extreme anisotropy of the mechanical, optical, and electrical properties of well-aligned materials. By comparison with small-molecule counterparts, nematic solutions of rodlike chains exhibit higher viscosities, along with pronounced viscoelastic behavior.[1,2] The focus here is to discuss a limited range of topics having to do with the viscoelastic properties. In the next section certain theoretical considerations are reviewed pertaining to special features of nematic fluids, including their texture (or defect structure) and their anisotropic viscoelastic properties. That is followed by a section on experimental observations, discussed in the perspective of theoretical expectations. In the former case, some of the discussion is specific to solutions of rodlike chains, but

[1] Department of Chemistry, Carnegie-Mellon University, Pittsburgh, Pennsylvania 15213.

0022-4715/91/0300-1041$06.50/0

much of the discussion applies to nematic fluids in general. The experimental observations are limited to the properties of nematic solutions of rodlike chains. Finally, a few concluding remarks are given.

2. THEORETICAL CONSIDERATIONS

2.1. Texture

The nematic phase is characterized by an orientation tensor **S** with components[1,3]

$$S_{\alpha\beta} = \langle u_\alpha u_\beta \rangle - \delta_{\alpha\beta}/3 \tag{1}$$

where **u** is a unit vector along the axis of a rodlike chain, δ is the unit tensor, and the angular brackets denote an ensemble average. At equilibrium, **S** may be expressed in terms of the director **n**, which is a unit vector along the symmetry axis. In general, the nematic phase may be characterized by an order parameter S given by[1,3]

$$S = [3\langle(\mathbf{u}\cdot\mathbf{n})^2\rangle - 1]/2 \tag{2}$$

It is presumed that S is everywhere the same when averaged over small volume elements, using **n** appropriate for each element, even though S computed using a globally averaged director might be small or zero for a defect-filled sample.

Nematic solutions of rodlike polymers may be prepared in a fully aligned (monodomain) form, with **n** everywhere the same.[4,5] Such preparations are not, however, common. Even though nematic solutions of rodlike polymers are fluids, they may be very viscous, leading to very slow attainment of the equilibrium alignment. In the later stages of the approach to equilibrium, the nematic fluid may exhibit texture in the form of slow, smooth changes in **n**, along with a few discontinuous changes in **n** comprising line or point defects (disclinations).[3] Disclinations have been reported for nematic solutions of rodlike polymers.[6-9] The disclinations contribute an excess free energy that may be analyzed through an elastic free energy density W, expressed for nematics as[3]

$$2W = K_S(\text{div}\,\mathbf{n})^2 + K_T(\mathbf{n}\cdot\text{curl}\,\mathbf{n})^2 + K_B(\mathbf{n}\times\text{curl}\,\mathbf{n})^2 \tag{3}$$

where K_S, K_T, and K_B are the Frank elastic constants for splay, twist, and bend distortions of the director field, respectively. Of course, defects are not found in fully aligned monodomains. Moreover, a constraint due to some agent extraneous to the sample must be present to support defects in a

well-annealed nematic fluid. For example, adsorption of the solute on the surfaces bounding a planar slab, with different orientations to the adsorbed layer in different domains on the surface, can give rise to a twisted nematic along the normal between the surfaces. The twist would develop to match the alignments at opposite surfaces, and could leave trapped disclinations at either surface.[10] Similarly, a line disclination could extend between pieces of debris on the surface, even though the director is otherwise uniform at the surface and throughout the bulk of the nematic. The effect of such defects has been studied by minimization of the total distortion free energy, computed as the integral of W over the sample volume.[3,10,11] Of course, estimates of the Frank elastic constants are necessary for such computations. Molecular theories express the elastic constants for rodlike chains of length L and diameter d in the form[12]

$$K_i = (kT/d)\, k_i(S, \hat{\rho}/L, \hat{\kappa}d, L_B/L_C) \tag{4}$$

with $i = T$, S, or B, and where the k_i are dimensionless functions of the indicated variables; here $\hat{\rho}$ is the persistence length of the rodlike contour, to account for deviation from a strict rod conformation,[13] and $\hat{\kappa}^{-1}$ is the Debye screening length for electrostatic interactions in a medium with Bjerrum length L_B for rods with charges spaced a distance L_C along the rod axis. It is often assumed that the k_i are equal, thereby affording a substantial simplification.[3] Unfortunately, this does not appear to be a reliable approximation for rodlike chains. For example, calculations based on the Onsager model for impenetrable cylinders[14] give numerical results that can be expressed as

$$k_T/k_S = 1/3 \tag{5}$$

$$k_B/k_S \approx 1.755\, \frac{1 - S/3}{1 - S} \tag{6}$$

$$k_S \approx 0.092 B_2 \nu (4S - 1) \tag{7}$$

Here, $B_2 = \pi L^2 d/4$ is the second virial coefficient (vol/molecule) and ν is the solute concentration (molecules/vol).[1] As discussed below, S depends on $B_2\nu$ for hard rods. The factor $1 - S$ in Eq. (6) causes K_B to diverge as S approaches unity. The effects of chain flexibility (small $\hat{\rho}/L$) and electrostatic interactions alter these expressions.[12,15-19]

As emphasized above, disclinations are observed in samples close to equilibrium. Under circumstances far from equilibrium the texture may be more complex and less well described. For example, a solution may be isotropic above some temperature T_{NI}, but nematic below T_{NI}, permitting

the formation of a highly nonequilibrium state by a rapid quench from above T_{NI} to well below T_{NI}. The situation immediately following the quench is akin to quenching a crystalline material from the melt to below its melting temperature. Thus, on quenching the nematogenic isotropic solution, multiple domains develop, each with order parameter S, but with no correlation of the alignment of the different domains. Such a sample is extremely turbid, unlike the fully aligned monodomain, and so far removed from equilibrium that the defect structure is ill defined, and does not exhibit the disclinations discussed above. (Wall defects that might be envisioned are not stable.[3,10] As discussed in the next section, similar textures far from equilibrium may develop in flow.

2.2. Viscoelastic Properties

In general, the linear viscoelastic theory of anisotropic fluids requires the use of a fourth-order tensor to express the stress tensor $\sigma(t)$ in the history of the strain tensor $\gamma(t)$ for an anisotropic fluid with a uniform director field.[20] As will be seen below, nematic solutions of rodlike polymers may be anisotropic at rest, requiring the use of such a theory to describe their behavior. Thus, in component form, the deviatoric stress is given by

$$\sigma_{ij}(t) \approx \int_{-\infty}^{t} G_{ijkl}(t-\theta) \frac{\partial \gamma_{kl}(\theta)}{\partial \theta} d\theta \tag{8}$$

where $\partial \gamma_{kl}/\partial t$ is the symmetric part of the velocity gradient tensor. A linearized form of a molecular model based on the evolution equation for the probability that a rodlike chain has orientation $\mathbf{u}$ at time t has been used to estimate $G_{ijkl}(t)$ for a nematic fluid in recently small deformations with the result[21]

$$\begin{aligned} G_{ijkl}(t) = 3\nu kTUS(1-S)[&2(\delta_{ik}\delta_{jl} - n_i n_k \delta_{jl} - n_j n_k \delta_{il} \\ &+ n_i n_j n_k n_l) \exp(-t/\lambda_2) \\ &+ n_i n_j n_k n_l (4S-1)(1+2S) \exp(-t/\lambda_1)] \end{aligned} \tag{9}$$

where ν is again the number concentration of polymer, $U = 3\nu/\nu_{NI}$, with ν_{NI} the value of ν required to make the isotropic state unstable relative to the ordered state, $\lambda_1^{-1} = 6\bar{D}_R US$, and $\lambda_1/\lambda_2 = (4S-1)/3$, with $\bar{D}_R$ the average rotational diffusion constant. For the model used, $\nu_{NI} = 16/\pi d L^2 = 4/B_2$,

$$4S = 1 + 3(1 - 8/3U)^{1/2} \tag{10}$$

for $U > 8/3$, and $\bar{D}_R$ is expressed in terms of the rotational diffusion constant $D_{R,0}$ at infinite dilution[1,22]:

$$\bar{D}_R = \beta D_{R,0}(\nu L^3)^{-2}(1-S^2)^{-2} \tag{11}$$

with β a constant. The linear steady-state shear viscosity η derived using Eqs. (8) and (9) is equal to that obtained in earlier, more direct calculations of η using the same model[1,22]:

$$\eta = \eta^{\mathrm{ISO}} \frac{(1-S)^4(1+S)^2(1+2S)(1+3S/2)}{(1+S/2)^2} \tag{12}$$

where $\eta^{\mathrm{ISO}} = (kT/6\beta)(\nu L^2)^3/D_{R,0}$. One feature of this result is that η decreases with increasing polymer concentration for nematic solutions near the phase boundary (ν a little larger than ν_{NI}). The model also predicts that the first-normal stress difference $\nu^{(1)}$ is proportional to the absolute value $|\kappa|$ of the shear rate, such that $\nu^{(1)}/|\kappa|$ may be expressed as a normal viscosity η_n, with[1,22]

$$\eta_n = \eta^{\mathrm{ISO}} \frac{3S(1-S)^{7/2}(1+S)^2(1+2S)^{1/2}}{1+S/2} \tag{13}$$

The model leading to Eqs. (12) and (13) has also been used to compute the Leslie–Ericksen viscosities α_μ appearing in the celebrated constitutive equation of Ericksen and Leslie,[23-25] which connects the deviatoric stress tensor σ with the deformation rate tensor κ. Thus, in component form in Cartesian coordinates, the viscous component of the stress tensor is given by[1,25]

$$\begin{aligned}\sigma_{ij} = {} & \alpha_1 n_k A_{kp} n_p n_i n_j + \alpha_2 n_i N_j + \alpha_3 N_i n_j \\ & + \alpha_4 A_{ij} + \alpha_5 n_i A_{jk} n_k + \alpha_6 A_{ik} n_k n_j\end{aligned} \tag{14a}$$

where the Einstein summation convention is employed, the α_μ are material constants (it generally being assumed that[26] $\alpha_6 = \alpha_2 + \alpha_3 + \alpha_5$), and

$$\mathbf{n} \times [\mathbf{h} - (\alpha_3 - \alpha_2)\mathbf{N} - (\alpha_2 + \alpha_3)\boldsymbol{A} \cdot \boldsymbol{n}] = 0 \tag{14b}$$

$$\mathbf{A} = \frac{1}{2}(\boldsymbol{\kappa} + \boldsymbol{\kappa}^+) \tag{14c}$$

$$\mathbf{N} = \frac{\mathbf{dn}}{dt} - \frac{1}{2}(\boldsymbol{\kappa} - \boldsymbol{\kappa}^+) \cdot \mathbf{n} \tag{14d}$$

with $\mathbf{n} \times \mathbf{h}$ the torque per unit volume arising from an external field or

spatial inhomogeneity of the director.[1,3,25] The Leslie–Ericksen viscosities are found to adopt the form[14,27,28]

$$\alpha_\mu = \eta^{ISO}(1-S^2)^2 H_\mu(S) \tag{15}$$

In fact, the same basic model has been treated with varying approximations to obtain differing estimates of $H_\mu(S)$.[27,28] A major difference is in the estimate of α_2/α_3, which is positive in the treatment leading to Eq. (12),[27] and negative in an alternative treatment.[28] In fact, since a uniform shear deformation obtains only if $\alpha_2/\alpha_3 > 0$,[3,25] this difference is rather striking. If uniform flow does obtain, then in the absence of other constraints, **n** adopts an orientation with **n** in the shear plane, but at angle $\theta_0 = \arctan(\alpha_3/\alpha_2)^{1/2}$ to the flow direction; θ_0 is called the Leslie angle.[3,25] A more complicated, and less well understood inhomogeneous flow is expected if $\alpha_2/\alpha_3 < 0$.[29] The effect of orientation imposed by the bounding surfaces on the flow has been studied within the frame of Eq. (14) for fluids with $\alpha_2/\alpha_3 > 0$.[30]

Of course, the splay, bend, and twist distortions discussed above have associated viscosities that may be expressed as combinations of the α_μ,[3,31]

$$\eta_T = \alpha_3 - \alpha_2 \tag{16}$$

$$\eta_S = \eta_T - 2\alpha_3^2/(\alpha_3 + \alpha_4 + \alpha_6) \tag{17}$$

$$\eta_B = \eta_T - 2\alpha_2^2/(\alpha_4 + \alpha_5 - \alpha_2) \tag{18}$$

These viscosities are of particular interest, since static and dynamic light scattering can be used to determine the ratios η_T/K_T, η_B/K_B, and η_S/K_S, as well as ratios of the Frank elastic constants.[3,31]

The (molecular) model leading to Eq. (12) has also been used to study the nonlinear dependence of the viscosity on shear rate κ.[33] The result gives the nonlinear viscosity η_κ in the form

$$\eta_\kappa = \eta_0 Q(\kappa/\bar{D}_R, S) \tag{19}$$

where η_0 is the limiting value of η_κ for small κ and S is the order parameter at equilibrium. In fact, flow is found to increase the order parameter with increasing $\kappa/\bar{D}_R$, with the effect occurring for smaller $\kappa/\bar{D}_R$ the smaller is S. In a different approach, certain nonlinear terms in the continuum theory for the Ericksen anisotropic fluid have been retained to explore transient behavior.[34] It appears, however, that this treatment results in certain nonphysical behavior.

The preceding has presumed the uniform flow predicted with the Ericksen–Leslie constitutive equation with positive α_2/α_3. In practice, as

discussed below, almost all experimental rheological studies on nematic solutions have been carried out starting with solutions far from the equilibrium texture. Consequently, there have been some attempts to model nematic fluids with a "domain" structure. Domains are sometimes considered to be regions of equilibrium order parameter, each domain with a characteristic orientation of the local director, but with no correlation among the alignment of the director among domains, giving an overall zero parameter.[35 37] In some cases, it is assumed that domains are bounded by disclination fields, and that these are the essential feature affecting the rheology in slow flows.[29,38] We will return to the discussion of domain structure below.

3. EXPERIMENTAL OBSERVATIONS

Experimental studies on nematic solutions of rodlike polymers are difficult, and suffer from several generic problems, including: (1) the limited availability of suitable model systems for rodlike polymers, i.e., chains for which the persistence length $\hat{\rho}$ exceeds L, (2) the tendency for interchain association in solutions of rodlike polymers, and the limited number of available solvents (often strong acids), and (3) the difficulty of obtaining (association-free) solutions of rodlike chains with a narrow distribution of chain lengths. Rodlike molecules studied include chains with the structures shown in Fig. 1. In most cases, the polymers studied have a molecular weight distribution with M_W/M_n no less than 1.5, and often larger. Of the structures presented above, PBG has the shortest persistence length. On the other hand, the first three may be dissolved only in strong acids (or equivalently reactive reagents). Thus, the first three are protonated in strong protic acids to form polyelectrolytes dissolved in solvents of varying ionic strength (depending on the acid, etc.). Usually, the ionic strength is high enough to substantially shield electrostatic interactions among the rodlike macroions. Questions of interchain associations are vexing, and not always appreciated. They may, for example, transform a nematic solution into an isotropic one under certain circumstances.[39]

In many cases, the flow curves (i.e., η_κ vs. κ) of nematic polymer solutions exhibit three regimes, as illustrated in Fig. 2. These are referred to hereafter as anomalous slow flow ($\eta_\rho R_0 \kappa < 0.1$), slow flow ($0.1 < \eta_P R_0 \kappa < 10$), and fast flow ($\eta_P R_0 \kappa > 10$). Here, η_P is the (nearly constant) viscosity observed in the slow flow regime, and R_0 is the limiting value of the steady-state recoverable compliance observed at small κ. These regimes will be considered individually in the following. First, however, we consider some experiments in which a magnetic field **H** is imposed on a monodomain nematic fluid to reorient the director. Such experiments are

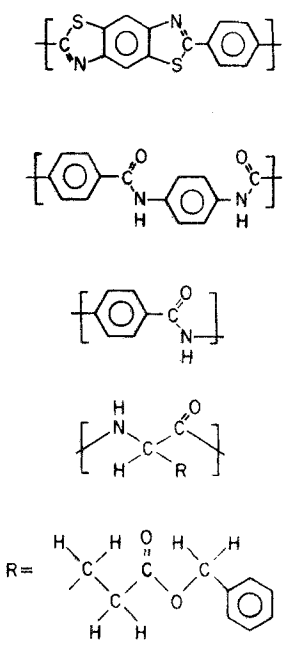

Fig. 1. Schematic structures for some rodlike chains: poly(1,4-phenylene-2,6-benzobisthiazole), PBT; poly(1,4-phenyleneterphthalamide), PPTA; poly(*p*-benzamide), PBA; and poly(γ-benzylglutamate), PBG.

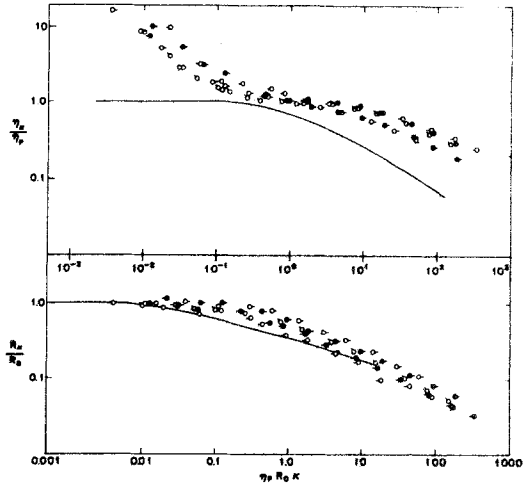

Fig. 2. Bilogarithmic plots of η_κ/η_P and R_κ/R_0 vs. $\eta_P R_0 \kappa$ for nematic solutions of PBT; the filled and unfilled circles represent data at two different temperatures and the pips denote solutions of different concentration. The curves represent similar functions for isotropic solutions, these reduced curves being independent of temperature. [From ref. 2.]

often used with small-molecule nematics to determine the Frank elastic constants from the critical value H_C of the magnetic field strength required to induce reorientation. Thus, a term $\Delta\chi(\mathbf{n}\cdot\mathbf{H})^2$ must be added to be rhs of Eq. (3), where $\Delta\chi$ is the anisotropic diamagnetic susceptibility of the solution.[3] With the addition of this term, the statics may be analyzed for particular orientations of the unit normal **s** to the sample slab (thickness b), the director **n**, and the magnetic field **H**, to obtain the K_i in terms of the critical field strength $H_{C,i}$ observed with each case[3]:

$$K_i = (bH_{C,i}/\pi)^2\,\Delta\chi \tag{20}$$

(e.g., $\mathbf{s}\cdot\mathbf{n}=\mathbf{n}\cdot\mathbf{H}=0$ and $\mathbf{s}\cdot\mathbf{H}=|\mathbf{H}|$ to measure K_S, $\mathbf{s}\cdot\mathbf{n}=\mathbf{n}\cdot\mathbf{H}=\mathbf{s}\cdot\mathbf{H}=0$ to measure K_T, and $\mathbf{s}\cdot\mathbf{H}=\mathbf{n}\cdot\mathbf{H}=0$ and $\mathbf{s}\cdot\mathbf{n}=1$ to measure K_B). With small-molecule nematics, the response to the applied field is rapid, but with nematic solutions of rodlike polymers the response is sluggish, and transient features develop that provide insight to the reorientation mechanism, as discussed in the next section.

3.1. Flow Induced by an External Magnetic Field

There have been a number of observations indicating that reorientations of the director in a fully aligned monodomain of rodlike chains in solution under the influence of a magnetic field may require reorientation coupled with flow.[2,40,42] Such conclusions are usually based on optical observations. For example, in studies on nematic solutions of PBG with the geometry used to measure K_T, bands are observed parallel to **H** in the early stages of the reorientation, with alternating large and small transmission $T_\perp(\psi'=0)$ for light transmitted between crossed polars. Here, ψ' is the angle between the polarizer and the original director $\mathbf{n}_0$.[40] Such nonuniform distortions are unexpected in the first order for H/H_C only slightly greater than unity according to the classical treatments.[3,31,43,44] The bands have a characteristic spacing $\lambda/2$ dependent on H/H_C. No features are reported for the transmission of polarized light without an analyzer for this system. The behavior has been analyzed with an analytic expression obtained[40] with a linearized form of Eq. (14), valid for the early stages of the distortion, as well as a numerical solution using the full expression in Eq. (14).[45,46] In both cases, it is assumed that the director remains everywhere parallel to the bounding surfaces, to obtain a relation between λ and H/H_C that depends on K_B/K_T, η_B/η_T, and η_c/η_a. In the latter, η_c is the viscosity with **n** parallel to the velocity gradient, and η_a is that with **n** perpendicular to both the flow direction and the velocity gradient [$2\eta_c=\alpha_4+\alpha_5-\alpha_2$ and $2\eta_a=\alpha_4$ with the use of Eq. (14)]. The solution

obtained has the reorientation coupled with planar circulatory flow patterns to produce a sinusoidal distortion of the director field, the amplitude of the distortion being zero at the boundaries and maximum in the plane halfway between the surfaces.

A more complicated behavior has been reported for PBT solutions under similar conditions.[2] In the latter case, incident light polarized along the original director produces alternating bright and dark bands parallel to **H** focused in planes a distance h above and below the center plane of the slab when the transmitted light is viewed without an analyzer (h may be smaller or greater than half the slab thickness); bright bands in the upper plane are above dark bands in the lower plane, and vice versa (see Fig. 3). The patterns are not observed with light polarized along **H**. In this case, Λ is initially independent of the field strength, by contrast to the behavior for λ discussed above, which varies in a complex way with H/H_c.[40] The separation of the two focal planes depends on both **H** and the time in the field. Although Λ is about independent of the time in the field initially, after some time, the interval suddenly decreases by half. These observations are attributed to cylindrical lenses formed by tilting of the director out of the plane of the slab as the reorientation proceeds, with the axes of the lenses parallel to **H** and spaced at more or less common interval $\Lambda/2$ along the original director. Thus, the reorientation is coupled with a nonplanar circulatory flow. The flow has been visualized by the motion of entrained motes (dust) in the solution under the influence of a magnetic field. In an analysis[45] of the periodic structures obtaining in the periodic in-plane distortion observed with PBG solutions, it was shown that these tend to periodic splay–bend inversion walls that are inherently unstable to out-of-

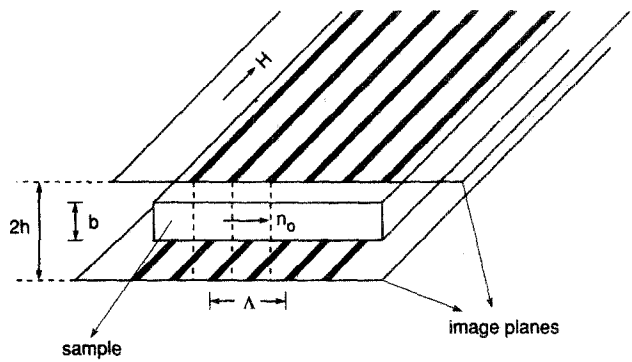

Fig. 3. Schematic drawing illustrating the alternating bright and dark stripes imaged in planes above and below the sample plane of symmetry for a nematic solution of PBT subjected to a magnetic field as viewed with incident light polarized along $\mathbf{n}_0$ (see text).

plane distortions of the director if $K_T \leqslant (K_S + K_B)/2$, so that the splay–bend inversion walls convert to twist walls at long time in the magnetic field—the latter would themselves be unstable to the development of disclination lines.[3,10] The observations made with PBT solutions may represent a transition of the in-plane splay–bend inversion walls to the predicted twist walls.

The preceding has focused on the application of relatively strong fields, leading to coupled reorientation and flow. It is of interest to consider the situation with field strength greater than H_C, and applied to a monodomain in the plane of the slab ($\mathbf{s}\cdot\mathbf{H} = \mathbf{s}\cdot\mathbf{n} = 0$) at a small angle to the undistorted director $\mathbf{n}_0$. In this case, one might expect to find a small, uniform distortion, such that the angle ϕ between $\mathbf{n}$ and $\mathbf{n}_0$ varied from zero at the surfaces (no distortion) to a maximum at the midplane of the slab. Thus, the angle $\phi(z, t)$ between the distorted and undistorted director at height z above the base surface in a slab of thickness b at time t following onset of the field may be evaluated by application of Eqs. (3) and (4).[3,44,47] For the conditions cited,

$$\phi(z, t) \approx \phi_M u(t/\tau_T) f(z/b) \tag{21}$$

where $\tau_T = \eta_T b^2/K_T$, and u tends to unity for large t. The relaxation following removal of the field after equilibrium is established is exponential[43,44]:

$$\phi(z, t') = \phi_M f(z/b) \exp(-\pi^2 t'/\tau_T) \tag{22}$$

where t' is the elapsed time following removal of the field. A method based on Eq. (22) utilizing nuclear resonance spectroscopy to follow u has been used to evaluate η_T/K_T for a nematic polyester.[47] Optical studies of the twist distortion require the use of polarized confocal optics to reveal the distortion. In this case, as illustrated in Fig. 4a, the interference figures characteristic of the undistorted uniaxial nematic are observed to rotate by an angle essentially equal to (1/2) $\arctan[\langle \sin 2\phi \rangle / \langle \cos 2\phi \rangle]$, where the average is over the slab thickness.[3,44] Such studies are underway for nematic solutions of PBT—it appears that a uniform distortion results under certain conditions (e.g., a small distortion angle).[48]

3.2. Behavior in Slow Flow

The flow behavior in the regime $0.1 < \eta_P R_0 \kappa < 10$ illustrated in Fig. 2 is usually observed for nematic solutions of rodlike polymers. Moreover, the viscosity η_P observed over this plateau is usually smaller than the (extrapolated) viscosity for an isotropic composition with the same

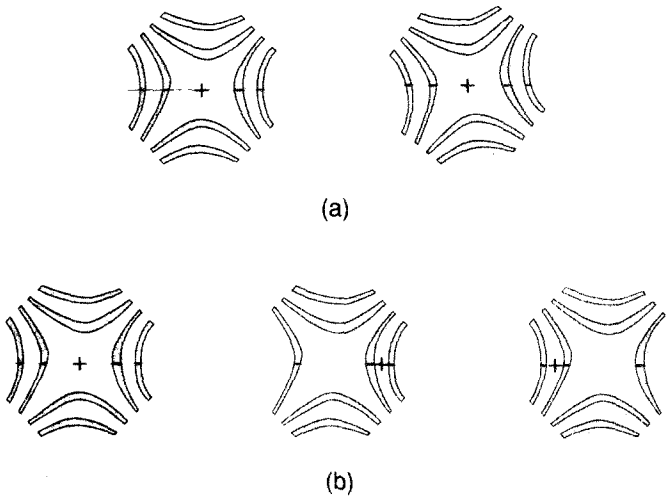

Fig. 4. Schematic drawing of interference figures obtained from a nematic solution of PBT under various circumstances. In these figures, the optic axis of the microscope is marked by a cross (+) and the original director is given by the dashed line. The polarizer and analyzer were crossed, and at about 45 deg to the original director (the latter angle is not critical, and does not affect the appearance of the interference figures except for their intensity). (a) The effect of a magnetic field in the twist geometry. Left, original; right, after exposure to a field (4.7 T) for 30 min, with the field in the sample plane and at an angle of 25 deg to the original director. (b) The effect of shear deformation along the axis of the original director. In this deformation, the lower plate was moved at velocity 10 μm/sec past the stationary upper plate, with a spacing of 250 μm between the two. From left to right the figures are before flow, and after the lower plate was displaced by 175 and 350 μm to the left, respectively. The interference figure returned to its original position at a displacement intermediate to the two given.

polymer concentration. These observations are in qualitative accord with the behavior discussed in connection with Eq. (12), etc., and appear to suggest a uniform flow in steady shear in the specified range of κ. Rheo-optical studies show that this is not the case for the solutions studied in Fig. 2,[2,8] and probably it is not the case for most of the rodlike solutions studied thus far.[49 51] In most cases, the flow is initiated on a solution with a director field far from equilibrium. For example, in such a case with a PBT solution,[2,8] during steady slow flow $T_+(\psi = \pi/4)$ was found to be very low on average (ψ being the angle between the polarizer and the flow direction), and to fluctuate in time, as did the transmission of polarized light measured without an analyzer. Moreover, in steady-state flow, the sample was turbid, quite unlike a fully aligned monodomain of the same solution at rest; the turbidity resulted in small transmission and low T_+. The mottled texture causing the turbidity is sometimes described as a polydomain,[35-37] in which the director is locally uniform in small

domains, but with no correlation of $\mathbf{n}$ among the domains, as in the "swarm model" of liquid crystals.[3,52] The actual situation is likely less compartmentalized, with the distortions continuous, but with a large gradient. Nevertheless, it is certain that for the systems cited, steady flow does not induce uniform alignment of the director under conditions of slow steady flow for which an essentially constant viscosity (i.e., η_P) is measured over a range of shear rate.

Relatively few experiments have been carried out with nematic solutions of rodlike chains in which flow is initiated on a monodomain. However, it is clear that in torsional flow of PBT solutions between parallel plates in the slow-flow shear-rate regime cited above, with the initial director along the radius, it was found[48] that the original (nearly) textureless solution became turbid after deformation by a few strain units, and remained turbid even after extensive strain in steady flow. Similar results have been observed with PBT solutions well oriented in a magnetic field prior to shear between two parallel plates along the axis normal to the director (the magnetic field being removed during shear)[48]—defect texture developed after only a few tenths of a strain unit. Remarkably, defect texture develops within one strain unit for the PBT solution studied if the flow axis and the original director are misaligned by as little as 4 deg. By contrast, no defect texture was observed after 10–20 units of shear strain if the shear was along the initial director. Nevertheless, as shown in Fig. 4b, conoscopic microscopy reveals that the director tilts in the shear plane in the latter flow. In this distortion the interference figure is observed to shift along an axis defined by the direction of the tilt of the principal optic axis, i.e., the offset center of symmetry of the interference figures is along the normal to the tilted director. Thus, for small strain, the observed distortion is consistent with the tilt expected for $\alpha_3/\alpha_2 > 0$. With increasing strain, the tilt reverses, becoming zero and then negative with increasing strain before the interference figures observed in conoscopy deteriorate. The original interference figures are recovered as the solution relaxes following cessation of flow. This behavior could indicate that α_3/α_2 changes sign with increasing S as S increases in flow, as expected with the treatment leading to Eq. (19). Related behavior has been observed with a small-molecule nematogen.[53-55] Alternatively, the unexpected transient behavior observed may reflect different relaxation times for the various anisotropic contributions to the stress. Experiments to verify this behavior and elucidate its dependence on the concentration and length of the rodlike chain are in progress.

Although estimates of η_B/η_T and η_S/η_T have been given for the PBT system[5] and a rather extensive study of these variables has been made for PBG,[56] the sign of α_2/α_3 is not known for either material—a reported

value[5] for PBT on the basis of measurements of η_B/η_T and η_S/η_T is fallacious owing to the double-valued nature of the square root.[57] Thus, it is not certain whether the optical behavior in steady flow might not be caused by nonuniform flow expected if $\alpha_2/\alpha_3 < 0$.

3.3. Behavior in Anomalous Slow Flow

As shown in Fig. 2, the stady-state viscosity increases with decreasing shear rate for very low κ (e.g., $\eta_P R_0 \kappa < 0.1$ in Fig. 2). This behavior is similar to effects observed in certain forms of yield from solid to fluid behavior. Nevertheless, studies on nematic solutions of PBT and PPTA show no yield behavior for the range of shear stress involved in anomalous flow.[2] Polydomain models have been evoked to rationalize the observed behavior, under the assumption that domains are defined by some kind of three-dimensional array of line disclinations. The domain size is calculated to be a function of the shear rate by a balance of viscous and elastic contributions, leading to a viscosity in slow flow that depends on the Frank elastic constants, and decreases with increasing shear rate.[29,38] As discussed above, a disclination texture develops slowly starting with a mottled nematic solution of rodlike polymers far from equilibrium. For this reason, it may be questionable whether the polydomain texture assumed in the preceding computation exists in practice.

An alternative origin for the behavior in anomalous slow flow, still related to elastic constraints, is that the effects of the alignment at the surface produce a stagnant boundary layer, with thickness δ dependent on the deformation velocity. Consequently, the torque and angular velocity measured in torsional deformation are not easily converted to a meaningful steady-state viscosity. Effects of this sort have been examined in detail for a number of geometries, in which the director field is initially uniform, but at some angle other than the Leslie angle θ_0 expected in steady shear flow (for $\alpha_2/\alpha_3 > 0$).[58] The results, calculated in the frame of the Leslie–Ericksen constitutive equation, give a steady-state viscosity η_δ (for $\alpha_2/\alpha_3 > 0$) that depends implicitly on δ:

$$\eta_\delta = \eta_0 \{1 - E^{-1/2} C(\theta_1, \theta_2, \theta_3, E)\}^{-1} \tag{23}$$

where η_0 is the viscosity calculated for uniform slow flow with $\delta = 0$, θ_1 and θ_2 are the alignment angles at the two surfaces in plane shear flow, and E is the appropriate Ericksen number $E_v = (\eta_v/K_v)\, Vh$ for splay, twist, or bend distortions, with V the relative velocity of surfaces separated by distance h. As seen in Eq. (23), $\eta_\delta \approx \eta_0$ if E is large, since then the viscous stress overwhelms the elastic one. In the discussion given earlier, η_B is

predicted to be smaller than η_S or η_T, and K_T diverges as $1-S$. Consequently, E_B is the smallest of the three Ericksen numbers, and surface effects involving E_B could reasonably result in enhanced η_δ. For the case of interest here, the alignment at the adsorbed surface layer is expected to be planar, but not uniform. Nevertheless, the propagation of the director alignment away from the surface can be expected to create a stagnant boundary layer of thickness that will decrease with increasing shear rate, consistent with the behavior seen in Fig. 2 for $\eta_P R_0 \kappa < 0.1$. The suggestion has not yet been given a definitive evaluation.

3.4. Behavior in Fast Flow

With $\eta_P R_0 \kappa > 10$, the steady-state viscosity η_κ decreases with increasing κ, consistent with Eq. (19), in which the order parameter increases with increasing κ. Nevertheless, rheo-optical experiments do not confirm the predicted uniform, well-aligned director field.[2,8,49,59] Thus, with the PBT solutions studied in Fig. 2, both the flow birefringence $T_+(\psi = 45)$ and transmission of polarized light (with no analyzer) fluctuated during steady fast flow, on a time scale smaller than κ^{-1}.[8] The length scale of the inferred fluctuations appears to decrease with increasing κ, as demonstrated by decreased apparent turbidity at larger κ. On cessation of flow $T_+(\psi = 45)$ tends to oscillate as the solution relaxes.[2,48] Such behavior is, however, not easily interpreted, and future observations should include conoscopy during relaxation on cessation of steady flow.

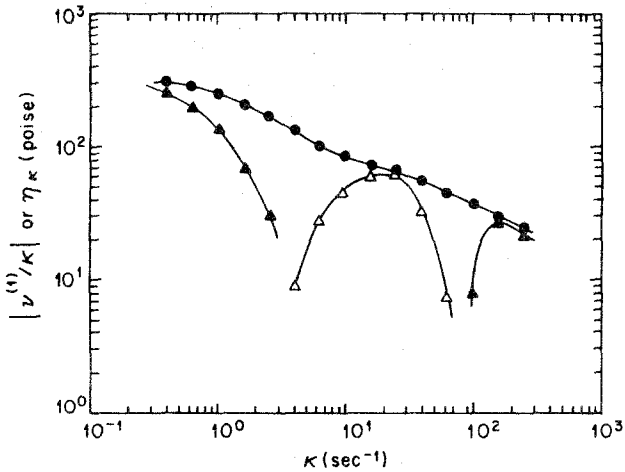

Fig. 5. The shear viscosity η_κ (circles) and the absolute value $|\nu^{(1)}/\kappa|$ of the normal viscosity η_n (triangles) as functions of the shear rate κ for a liquid crystalline solution of PBG; $\nu^{(1)}$ is positive for filled triangles and negative for unfilled trianges. [From ref. 2.]

Other unusual behavior observed with nematic solutions of rodlike chains include oscillations in the shear stress on the initiation of flow at constant rate, and a first-normal stress difference $\nu^{(1)}$ that oscillates between positive and negative values with increasing shear rate in steady flow. The latter is illustrated in Fig. 5 for data on a nematic solution of PBG[60]. Remarkably, the absolute value $|\nu^{(1)}/\kappa|$ of the normal viscosity tends to η_κ for the maximum $|\nu^{(1)}/\kappa|$. As mentioned above, a normal viscosity $\eta_n = \nu^{(1)}/|\kappa|$ is predicted with the Leslie-Ericksen constitutive relation [e.g., see Eq. (13)]. Although negative $\nu^{(1)}$ have been predicted in homogeneous slow flow due to the effects of surface alignment,[61] oscillatory behavior is not predicted and the observed negative $\nu^{(1)}$ in fast flow probably has a different origin. Oscillatory behavior on the initiation of fast flow at constant rate has been reported for both the shear stress and $T_+(\psi = 45)$.[8,49] Typically, oscillations in the shear stress persist for strain κt less than about 100, and depend on the prior strain history. As mentioned above, higher frequency oscillations in the flow birefringence persist even when the stress is steady. The oscillatory behavior, so far unexplained, may be caused by the onset of tumbling of the director, eventually leading to a complex, nonuniform flow.

4. CONCLUSION

Some of the salient features observed in the flow behavior of nematic solutions of rodlike chains have been discussed in contrast with theoretical predictions based on a constitutive equation devised for low-molecular-weight nematogens. Although yet incomplete, studies on the deformation of well-aligned monodomains appear to reveal discrepancies between the observed and predicted behaviors. Furthermore, it seems unlikely that the flow behavior of the more commonly studied defect-filled textures can be described by the available theory.

ACKNOWLEDGMENT

Preparation of this manuscript was supported in part by a grant from the National Science Foundation, Polymers Program.

REFERENCES

1. M. Doi and S. F. Edwards, *The Theory of Polymer Dynamics* (Clarendon Press, Oxford, 1986).
2. G. C. Berry, *Mol. Cryst. Liq. Cryst.* **165**:333 (1988).
3. P. G. de Gennes, *The Physics of Liquid Crystal* (Clarendon Press, Oxford, 1974).

4. S. Fraden, A. J. Hurd, R. B. Meyer, M. Cahoon, and D. L. D. Caspar, *J. Phys.* (Paris) (Suppl. C3), 85 (1985).
5. K. Se and G. C. Berry, *Mol. Cryst. Liq. Cryst.* **153**:133 (1987).
6. M. Panar and L. F. Beste, *Macromolecules* **10**:1401 (1977).
7. Y. Onogi, J. L. White, and J. F. Fellers, *J. Polym. Sci. Phys. Ed.* **18**:663 (1980).
8. G. C. Berry, K. Se, and M. Srinivasarao, in *High Modulus Polymers*, A. E. Zachariades and R. S. Porter, eds. (Marcel Dekker, New York, 1988), p. 195.
9. V. G. Kulichikhin, V. A. Platonov, L. P. Braverman, T. A. Belousom, V. F. Polyakov, M. V. Shablygin, A. V. Volokhina, A. Ya. Malkin, and S. P. Papkov, *Polym. Sci. USSR* **18**:3031 (1977).
10. M. Kléman, *Points, Lines and Walls* (Wiley, New York, 1985).
11. A. Saupe, *Mol. Cryst. Liq. Cryst.* **21**:211 (1973).
12. T. Odijk, *Macromolecules* **19**:2313 (1986).
13. H. Yamakawa, *Modern Theory of Polymer Solutions* (Harper and Row, New York, 1971).
14. S.-D. Lee and R. B. Meyer, *J. Chem. Phys.* **84**:3443 (1986).
15. P. G. de Gennes, *Mol. Cryst. Liq. Cryst. Lett.* **34**:177 (1977).
16. A. Yu Grosberg and A. V. Zhestkov, *Polym. Sci. USSR* **28**:97 (1986).
17. T. Odijk, *Liq. Cryst.* **1**:553 (1986).
18. G. J. Vroege and T. Odijk, *J. Chem. Phys.* **87**:4223 (1987).
19. S.-D. Lee and R. B. Meyer, *Phys. Rev. Lett.* **61**:2217 (1988).
20. R. M. Christensen, *Theory of Viscoelasticiy*, 2nd ed. (Academic Press, New York, 1982), p. 5.
21. R. G. Larson and D. W. Mead, *J. Rheol.* **33**:185 (1989).
22. M. Doi, *J. Polym. Sci. Phys. Ed.* **19**:229 (1981).
23. J. L. Ericksen, *Arch. Rat. Mech. Anal.* **4**:231 (1960).
24. F. M. Leslie, *Arch. Rat. Mech. Anal.* **28**:265 (1968).
25. F. M. Leslie, *Adv. Liq. Cryst.* **4**:1 (1979).
26. O. Parodi, *J. Phys.* (Paris) **31**:581 (1970).
27. G. Marrucci, *Mol. Cryst. Liq. Cryst.* **72**:153 (1982).
28. N. Kuzuu and M. Doi, *J. Phys. Soc. Japan* **52**:3489 (1983); **53**:1031 (1984).
29. G. Marrucci, *Pure Appl. Chem.* **57**:1545 (1985).
30. P. K. Currie, *J. Phys.* (Paris) **40**:501 (1979).
31. S. Chandrasekhar, *Liquid Crystals* (Cambridge University Press, Cambridge, 1977).
32. M. Doi, in *Theory and Applications of Liquid Crystals*, J. L. Ericksen and D. Kinderlehrer, eds. (Springer-Verlag, New York, 1987), p. 143.
33. A. B. Metzner and G. M. Prilutski, *J. Rheol.* **30**:661 (1986).
34. G. G. Viola and D. G. Baird, *J. Rheol.* **30**:601 (1986).
35. T. Asada, in *Polymer Liquid Crystals*, A. Ciferri, W. R. Krigbaum, and R. B. Meyer, eds. (Academic Press, New York, 1982), Chapter 9.
36. V. G. Kulichikhin, N. V. Vasil'yeva, V. A. Platonov, A. Ya. Malkin, T. A. Belousova, O. A. Khanchich, and S. P. Papkov, *Polym. Sci. USSR* **21**:1545 (1980).
37. K. F. Wissbrun, *J. Rheol.* **25**:619 (1981).
38. K. F. Wissbrun, *Faraday Disc. Chem. Soc.* **79**:161 (1985).
39. K. Se and G. C. Berry, in *Reversible Gels and Related Systems*, P. S. Russo, ed. (American Chemical Society Symposium Series, 1987), p. 129.
40. F. Lonberg, S. Fraden, A. J. Hurd, and R. B. Meyer, *Phys. Rev. Lett.* **52**:21, 1903 (1984).
41. C. R. Fincher, Jr., *Macromolecules* **19**:2431 (1986).
42. Y. W. Hui, M. R. Kuzma, M. San Miguel, and M. M. Labes, *J. Chem. Phys.* **83**:288 (1985).
43. F. Brochard, P. Pieranski, and E. Guyon, *Phys. Rev. Lett.* **28**:1681 (1972).

44. P. E. Cladis, *Phys. Rev. Lett.* **28**:1629 (1972).
45. A. D. Rey and Morton M. Denn, *Liq. Cryst.* **4**:409 (1989).
46. G. Srajer, S. Fraden, and R. B. Meyer, *Phys. Rev. A.* **39**:4828 (1989).
47. A. F. Martins, P. Esnault, and F. Volino, *Phys. Rev. Lett.* **57**:1745 (1986).
48. M. Srinivasarao, to be published.
49. P. Moldenaers, G. Fuller, and J. Mewis, *Macromolecules* **22**:960 (1989).
50. G. Marrucci, N. Grizzuti, and A. Buonaurio, *Mol Cryst. Liq. Cryst.* **153**:263 (1987).
51. B. Ernst and P. Navard, *Macromolecules* **22**:1419 (1989).
52. L. S. Ornstein and W. Kast, *Trans. Faraday Soc.* **29**:931 (1933).
53. K. Skarp, T. Carlsson, I. Dahl, S. T. Lagerwall, and B. Stebler, in *Advances in Liquid Crystal Research and Applications*, L. Bata, ed. (Pergamon Press, Oxford, 1980), p. 573.
54. Ch. Gähwiller, *Phys. Rev. Lett.* **28**:1554 (1972).
55. P. Pieranski, E. Guyon, and S. A. Pikin, *J. Phys.* (Paris) **37Cl**:3 (1976).
56. V. Taratuta, A. J. Hurd, and R. B. Meyer, *Phys. Rev. Lett.* **55**:246 (1985).
57. W. Burghardt, Private communication.
58. P. K. Currie, *Rheol. Acta* **16**:205 (1977).
59. H. L. Doppert and S. J. Picken, *Mol. Cryst. Liq. Cryst.* **153**:109 (1987).
60. G. Kiss and R. S. Porter, *Mol. Cryst. Liq. Cryst.* **60**:267 (1980).
61. P. K. Currie, *Mol. Cryst. Liq. Cryst.* **73**:1 (1981).